

Super Absorbent Hydrogel Derived from Activated Charcoal Functionalized with Ethylenediamine and Cross-linked with Maleic Acid

Titus M. Kasimu¹, Harun M. Mbuvi¹, Francis M. Maingi^{2,*}

¹Department of Chemistry, Kenyatta University Nairobi, Kenya

²Department of Science Technology and Engineering, Kibabii University Bungoma, Kenya

Abstract Superabsorbent hydrogels represent a set of polymeric materials with three-dimensional networks capable of holding a huge amount of water due to their hydrophilic nature in their structure. Their application in industries and the environment is of prime importance. This study reports the synthesis and characterization of superabsorbent hydrogels derived from activated charcoal. The activated charcoal (AC) was functionalized with ethylenediamine (EA) using sodium hydroxide as a catalyst in the absence and presence of maleic acid as a cross linker to synthesize HCE-1 and HCE-2 superabsorbent hydrogel respectively. Characterization of the hydrogels was done using Fourier transform infrared (FT-IR) spectroscopy, scanning electron microscope (SEM), and X-ray diffraction (XRD). The synthesis conditions producing optimal swelling capacity were studied by varying contact time and dosage of both activated carbon and the maleic acid. The results showed presence of C-N- stretching vibration at 1590.99 cm^{-1} in FT-IR spectrum of HCE-1 indicating interlinking between AC and EA monomers. XRD analysis showed a shift from amorphous to crystalline upon crosslinking. SEM analysis showed dense mast homogenous morphology with clear pores network in HCE-2 compared to the rigid rough surface observed in HCE-1 hydrogel. The dose ratio of AC: EA: maleic acid of 6:5:2 produced hydrogel with highest water absorption capacity of $1089.7 \pm 0.6\%$. Crosslinking the hydrogel with maleic acid was found to improve the water absorption capacity of the absorbent. The study provides a baseline for the application of the hydrogel in agriculture, especially in semi and arid regions.

Keywords Activated charcoal, Characterization, Crosslinking, Ethylenediamine, Superabsorbent hydrogel

1. Introduction

Absorbent hydrogels are 3D lattice polymers with cross-linked hydrophilic functional groups and are insoluble in water [1]. They can absorb and retain water at least 400 times its original weight. They also make at least 95 percent of their stored water available for absorption [2]. Hydrogels are usually prepared from polar materials and are classified as physically and chemically cross-linked gels. Physically, cross-linked gels have their networks held together by physical forces, including ionic, H- bonding, or hydrophobic forces, while chemically cross-linked gels have covalently cross-linked networks [3]. Most of the hydrogels reported in the literature are synthetic non-biodegradable organic compounds [4]. This becomes the driving force for researchers to develop superabsorbent hydrogels from locally available natural materials which are degradable

especially starch and chitosan among others [5]. Hydrogels have varied applications. Most common are; hygiene napkins, disposal diapers, soil for horticulture and agriculture, water and food purification [6]. Currently, hydrogels are applied mostly in technological fields including medicine [3], agriculture and horticulture [7], food packaging [8], and wastewater treatment [5]. These materials can absorb water 20 times more than their weights and are therefore referred to as super-absorbent [9]. Low-cost hydrogels with high swelling capacities have attracted more emphasis in the field of agriculture [10]. This study was geared towards the synthesis of super hydrogel absorbers from biodegradable materials for possible application in agriculture. The main chain polymer was obtained through interlinking carboxylate functional groups in AC and amine groups in EA. The maleic acid was used as a binding molecule between the polymeric units formed through ester cross-linkage. The hydrogel formed will have an increased number of hydrophilic groups and hence resulting in increased water absorption capacity.

* Corresponding author:

mukoramaingi@yahoo.com (Francis M. Maingi)

Received: Dec. 13, 2021; Accepted: Dec. 27, 2021; Published: Jan. 13, 2022

Published online at <http://journal.sapub.org/ijmc>

2. Materials and Methods

2.1. Reagents and Chemicals

The Coconut shells were obtained from Mombasa County-Kenya and transported to Kenyatta University laboratory. Ethylenediamine used was obtained from Merck Chemical Co (Darmstadt, Germany), potassium manganate VII, sodium hydroxide, and sulphuric acid were obtained from Kenya science chemical limited Kenya, while maleic acid was obtained from Sigma Aldrich Company (Germany).

2.2. Preparation of Activated Carbon

The preparation procedure of activated charcoal was adopted from Papita [11]. Pieces of dry coconut shells were placed into a 20-L aluminum container and excess air was removed by warming. The container was then tightly closed and heated at a temperature of 473 to 553K for 8 hours after which cooling was done for 24 hours to obtain carbonized charcoal [11]. The charcoal was crushed and grounded into powder using a Sheller machine (Honda ESB 501). 20 g of the powdered charcoal was then put in a 1 L Erlenmeyer flask and 500 mL of 2M solution of acidified potassium permanganate was added. The mixture was allowed to stand for 12 hours to oxidize carbon. Oxidative reaction introduces oxygen functional groups on the surface of carbon materials to enhance functionalizing ability with ethylenediamine [9]. The mixture was then filtered and the residue was washed with deionized water to remove the purple color of the oxidizing agent and air-dried in the open to a constant weight to obtain activated carbon.

2.3. Functionalization of Activated Carbon with Ethylenediamine to Form Hydrogel HCE-1

The procedure for the functionalization of activated charcoal with ethylenediamine was adopted from Basri *et al.* [12] with slight modification. The process occurred through interlinking the carboxylic acid group in AC with the amine group in EA to form a monomeric unit through an amide linkage. Accurately weighed 80.0 g of powdered AC using a weighing balance with precision (CZ 200) was transferred to a 1000 mL Erlenmeyer flask. 150 mL of deionized water was then added while stirring to form a carbon suspension. The obtained mixture was heated to a temperature of 100°C for 5 minutes followed by the addition of 50.0 g of ethylenediamine and 2.0 g of sodium hydroxide pellets as the activator. The heating of the resultant mixture at a temperature of 150°C was done until a paste formed, after which it was allowed to cool to room temperature to form a solid hydrogel polymer labeled HCE-1.

2.4. Crosslinking the Hydrogel HCE-1 with Maleic Acid

The cross-linked HCE-2 superabsorbent hydrogel was prepared by adding 10.0 g of maleic acid to boiling HCE-1. Stirring and heating of the mixture was done continuously at a temperature of 150°C until viscous gel was formed. The gel was then cooled at room temperature to form superabsorbent

hydrogel labeled HCE-2. Ester linkage was facilitated by the availability of hydroxyl groups in the polymeric material HCE-1 and carboxylate groups in maleic acid. Figure 1 shows the diagrammatic scheme for the preparation of the hydrogel.

2.5. Characterization of the Hydrogel

2.5.1. Fourier Transform Infrared (FT-IR) Analysis of the Superabsorbent Hydrogels

The procedure was adopted from Demitri *et al.* [13] to determine functional groups present in the hydrogels absorbers. Crystal of the superabsorbent hydrogels with and without cross-linker HCE-2 and HCE-1 respectively were dried in the open air for 12 hours until they attained constant weight. 1 mg of each of the hydrogel was mixed with 25 mg of dry spectroscopic grade potassium bromide. The mixtures were ground using pestle and mortar to form a fine powder. The powder was compressed into thin pellets and investigated for functional groups using FT-IR (Shimadzu IR Tracer-100) at a wavelength range of 4000-200cm⁻¹ [14].

2.5.2. Phase Composition Analysis of the Superabsorbent Hydrogels

The procedure for phase analysis of the hydrogels HCE-1 and HCE-2 was adopted from Wanrosli *et al.* [15]. Analysis was done using XRD (Hossein Beygin) at scattering angle (2θ) ranging from 10 to 90° and at a scan rate of 5°/min.

2.5.3. Microstructural Analysis of the Superabsorbent Hydrogels

The microstructural analysis of HCE-1 and HCE-2 hydrogel was determined by soaking them in buffer solutions of pH 11 for 12 hours. The mixture was then filtered using filter paper no 41 and residue dried in the oven at 45°C until a constant weight was obtained. Dried hydrogels were coated with gold. The gold-plated stubs were then placed in a SEM chamber (Zeiss Supra 60) at an accelerating voltage of 250 kV to obtain SEM micrographs [16].

2.6. Effect of Mass of AC (g) on the Swelling Capacity of Cross-linked Hydrogel

The hydrogels were prepared by varying mass of AC from (1, 2, 4, 6, 8, and 10 g) while maintaining the mass of ethylenediamine at 5.0 g, maleic acid binder at 2.0 g, and 1.0 g of NaOH activator. 2.0g of each prepared sample was then immersed in water for 24 hours to determine the swelling capacity.

2.7. Effect of Cross-linker on the Swelling Capacity of the Hydrogel

The effect of the cross-linker was studied in triplicates by varying the mass of maleic acid (0.5, 1.0, 1.5, 2.0, 2.5, and 3.0 g) while maintaining the mass of activated carbon as 6 g, the mass of ethylenediamine as 5.0 g, and the mass of sodium hydroxide activator as 1.0g. 2.0 g of each prepared sample

was then immersed in water for 24 hours to determine the swelling capacity as described in equation 1 provided in section 2.9.

2.8. Effect of Swelling Time on the Swelling Capacity of the Hydrogel HCE-2

The effect of swelling time on swelling of superabsorbent hydrogels HCE-2 was studied in triplicates by varying time

(0.5, 1, 2, 4, 6, 12, and 24 hours). 2.0 g of each hydrogel prepared at the optimum ratio of AC: EA: maleic acid of 6:5:2 was immersed in 500 mL for a specified swelling time. The samples were then periodically removed after the expiry of contact time and its new mass determined. The swelling capacity was then determined using equation 1 provided in section 2.9.

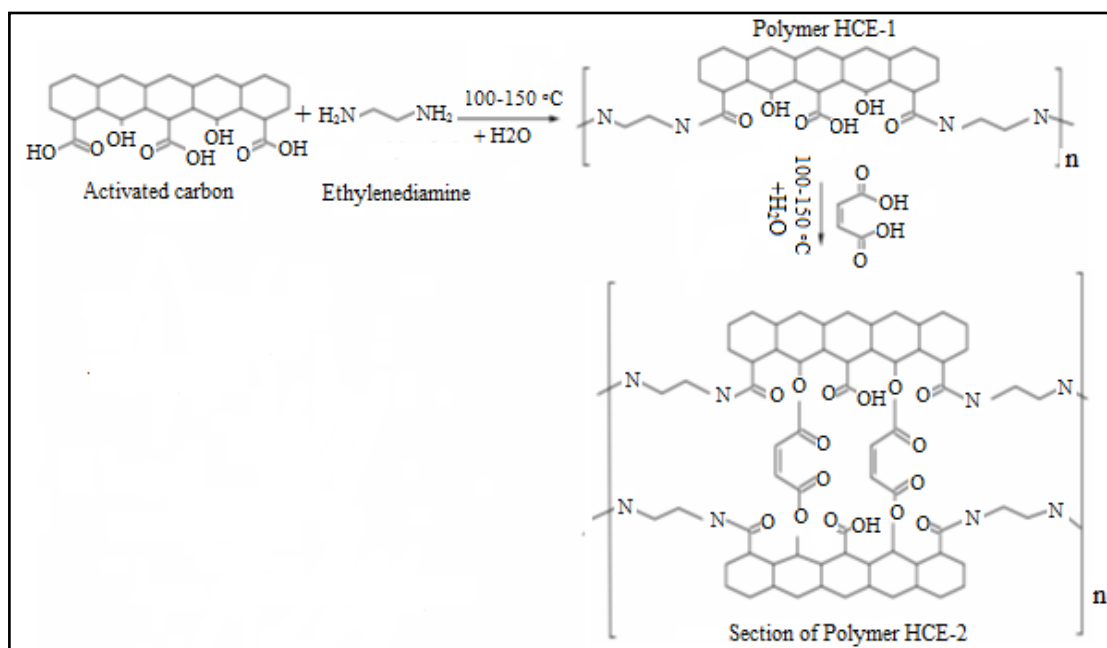


Figure 1. Diagrammatic scheme for the preparation of hydrogel

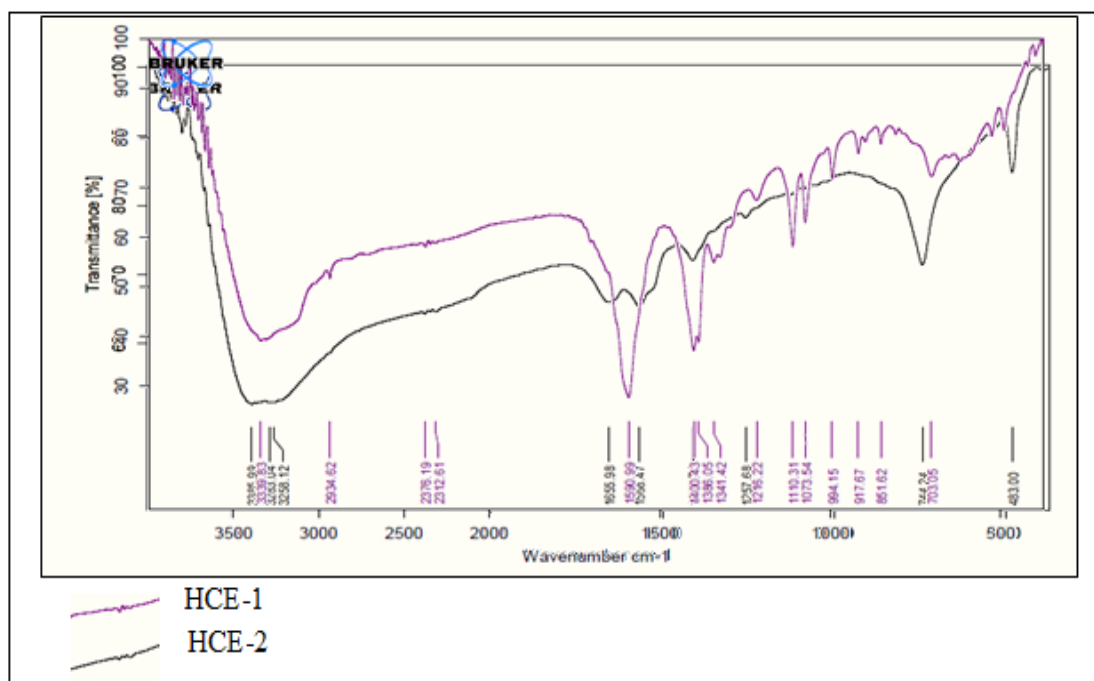


Figure 2. FT-IR Spectrum of HCE-1 and HCE-2 hydrogels

2.9. Equilibrium Water Content (EWC)

The procedure for determining equilibrium water content (EWC) was adopted from [16]. 2.0 g of the hydrogel polymers were put in polyester bags. The weight of the hydrogels and polyester bags was determined and recorded as (W_s). The polyester bags containing hydrogels were then immersed in 500 mL of distilled water and allowed to absorb water for 24 hours. After the swelling period, the samples were removed and excess water on the surface of polyester bags was removed using tissue paper and their weight determined and recorded as (W_d) [16]. Equation 1 was used to determine the equilibrium water content.

$$EWC(\%) = \frac{W_s - W_d}{W_d} \times 100 \quad (1)$$

Where W_s is the initial weight of hydrogel before swelling and W_d is the final mass of hydrogel after swelling.

3. Results and Discussions

3.1. FT-IR Spectrum of Superabsorbent Hydrogels

Analysis using FT-IR was carried out to identify the functional groups present in hydrogel super absorbers before and after cross-linking. Figure 1 shows the IR spectrum of the uncross-linked hydrogel HCE-1 and cross-linked hydrogel (HCE-2).

Figure 2 shows the FT-IR spectrum of HCE-1 and HCE-2 hydrogels. The absorption peaks in HCE-1 observed at around 3339.83 cm^{-1} and 2934.62 cm^{-1} were attributed to -OH stretching vibration and C-H asymmetric stretching of methylene in AC [17]. The sharp spectra bands at 1590.99 cm^{-1} , 1216.2 cm^{-1} in HCE-1 were associated with C-N-stretching vibration and N-H bending bond, indicating an

interlink between AC and EA monomers [18]. Peaks appearing at around 1341.4 cm^{-1} , 1073.5 cm^{-1} were due to -OH bending and C-O- stretching vibration in HCE-1 respectively [19]. In addition, IR peaks at 1400.43 cm^{-1} and 1386.05 cm^{-1} were assigned to -COO- carboxylate group associated with AC in the gel. Broad sharp peaks at 1110 cm^{-1} , 994 cm^{-1} , 917.7 cm^{-1} , and 703 cm^{-1} were due to alkyl substitutes in ether C-O stretching, vinyl C-H out of plane bending, bending -OH vibration, and bonding deformation vibration respectively [20]. The spectra band at a wavelength around 851.6 cm^{-1} and 703.05 cm^{-1} was a relatively pure ring stretching mode associated with aromatic ether C-O-O- and H bond deformation in AC [21], [22]. The peaks in HCE-2 appearing at 3283.04 cm^{-1} , 3258.12 cm^{-1} were associated with normal polymeric -OH stretching in AC overlapping with asymmetric strong H bond interaction in EA [17]. The appearance of sharp peaks at 3385.99 , 1257.68 cm^{-1} , and 744.24 cm^{-1} were accredited to broad -OH stretching vibration, -OH phenolic bending, and -OH bending in carboxylate respectively [23]. The increased presence of hydrophilic groups shows increased water affinity on the surface of HCE-2. A shift in the peak from 1386.05 to 1411.73 cm^{-1} -COO- stretching vibration could be attributed to the ester crosslink between the polymer chains of HCE-1 gel to form an HCE-2 hydrogel [24].

3.2. Phase Composition of HCE-1 and HCE-2 Hydrogels

Figures 3 and 4 show the diffraction patterns of super hydrogel absorbers HCE-1 and HCE-2 respectively obtained during the analysis. The amorphous hump observed between angle (2θ) 10 and 31° in figure 3 and the few crystalline phases shows that HCE-1 was semi-crystalline [25].

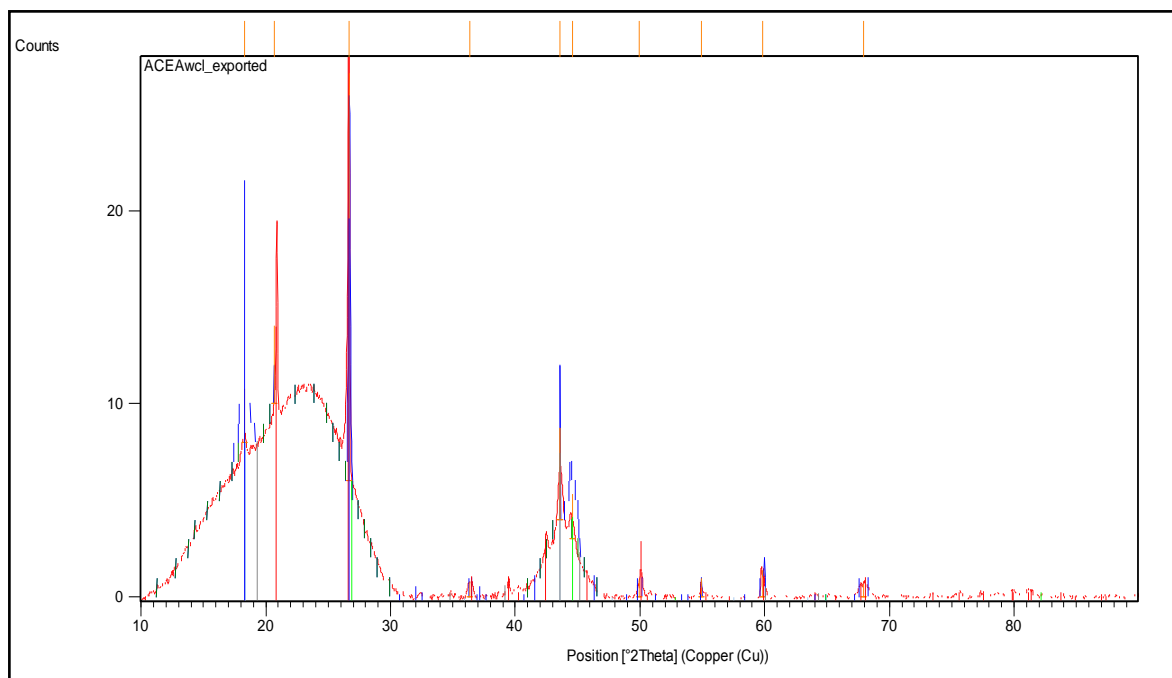


Figure 3. Powdered diffraction pattern of HCE-1 Hydrogel

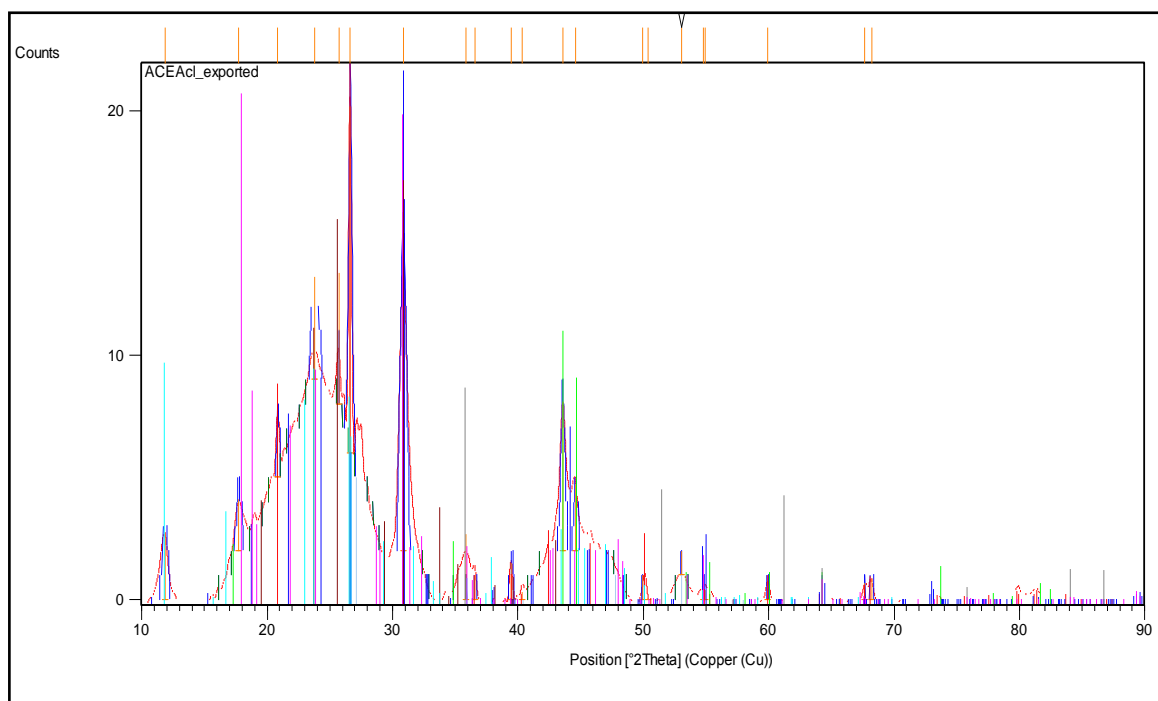


Figure 4. Powdered diffraction pattern of HCE-2 hydrogel

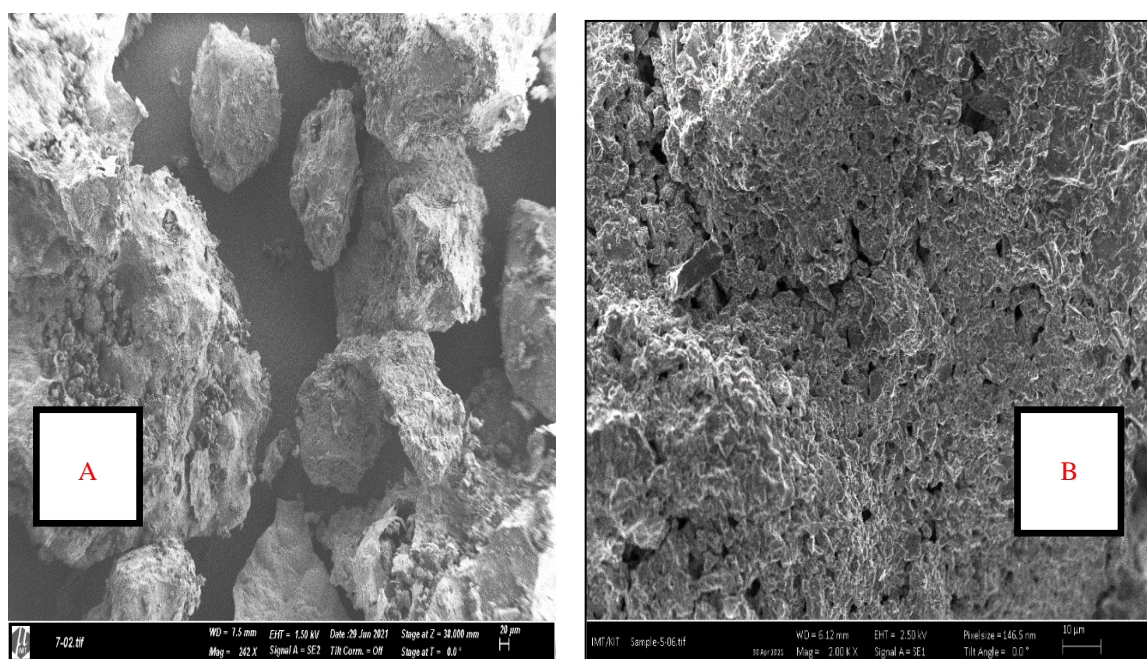


Figure 5. SEM micrographs of HCE-1 (A) and HCE-2 (B) hydrogels

Upon crosslinking the hydrogel became more crystalline as more sharp peaks were observed (Figure 4).

New peaks appeared on HCE-2 hydrogel at 2θ values of 23.81 and 25.71 due to the tubular structure of carbon atoms in the hydrogel [26]. The sharp, well-resolved peaks at angle 2θ 30.84, 35.88, 39.45 confirmed crystalline phases of graphite, carboxylate, and amine respectively. The peaks at an angle (2θ) of 40.33 and 50.37 were due to the crystalline phase structure of the hydrogel [27]. The peak at 18.27(2θ) (Figure 4) associated with a crystalline phase of N-C=O in

HCE-1 disappeared upon cross-linking. This could be attributed to the fact that there were inter and intramolecular interactions between $-\text{COOH}$ in AC and $-\text{NH}_2$ group from EA forming a strong crystalline phase network in HCE-2 super hydrogel [28]. A higher degree of crystallinity was observed in HCE-2 super hydrogel as compared to HCE-1. XRD analysis shows an increase in crystallinity upon binding and this is key towards hydrogel degradability, water uptake, and swelling ratio [29].

3.3. Analysis of Microstructure in the Hydrogel Using Scanning Electron Microscope (SEM)

The microstructure and morphological analysis of the hydrogel absorbers of HCE-1 and HCE-2 was done using a scanning electron microscope (SEM) (model Zeiss supra 60) at an accelerating voltage of 2.50 kV. The SEM images of powdered hydrogels are shown in figure 5.

The micrographs show the presence of voids due to the irregular continuous mass of particles that are compacted in the gels. The micrograph of HCE-2 shows dense mast homogenous morphology compared with the rigid rough morphology of HCE-1. This could be attributed to complete polymerization that occurred upon the addition of the crosslinker [30]. The HCE-2 consists of tubular vitreous networks which are spheres that are hollow containing

microspheres that are linked to the inner part of the larger spherical particles [31]. This revealed that the addition of cross linker facilitated polymerization reaction via formation of ester links, more cross linker points, and increased crosslinking density on hydrogel resulting in the formation of rough and protrusions surfaces throughout the micrographs which are responsible for water absorption [32].

3.4. Effect of Amount of AC Used on the Swelling Capacity of Hydrogel (HCE-2)

Figure 6 shows the mean percentage swelling obtained when 2.0 g of prepared hydrogel was immersed in distilled water as described in section 2.6.

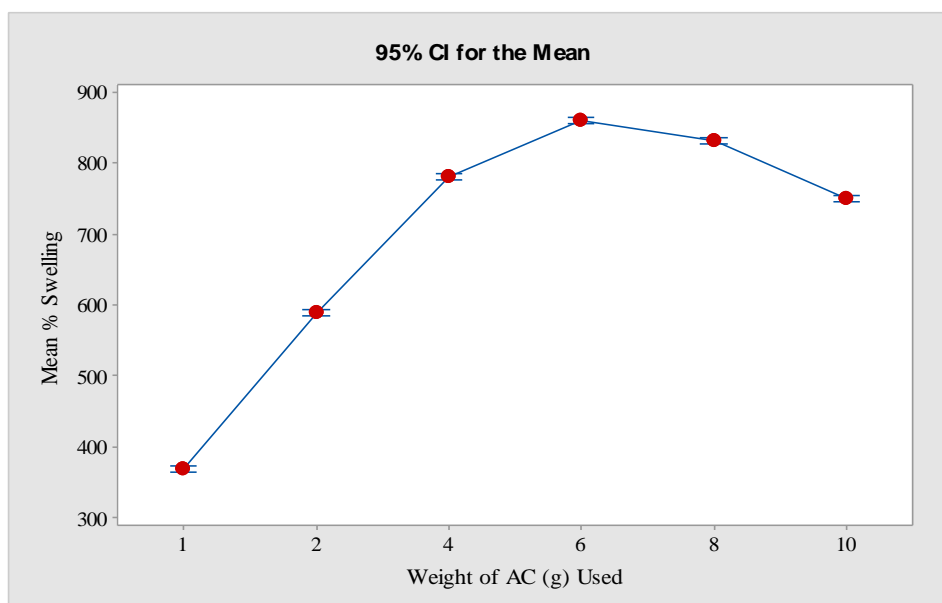


Figure 6. Effect of amount of AC (g) on % swelling of 2 g of HCE-2

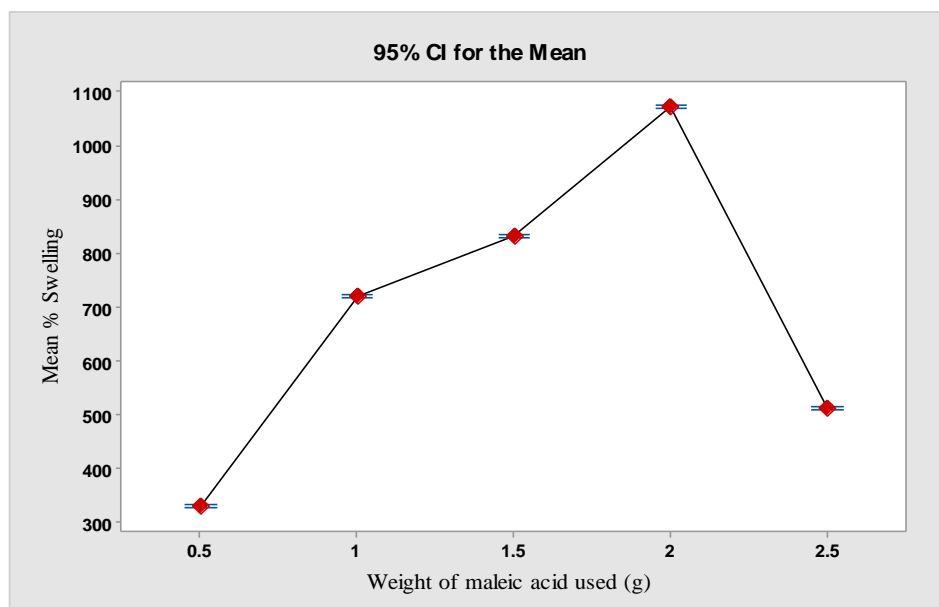


Figure 7. Effect of weight of maleic acid (g) on % swelling of HCE-2

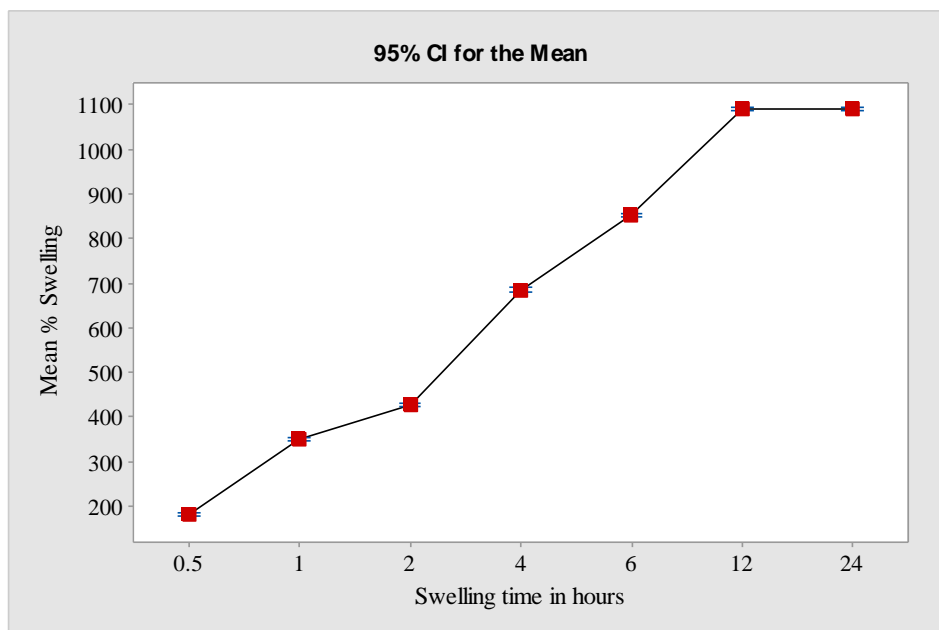


Figure 8. Effect of swelling time on % swelling of 2 g of HCE-2 at optimum ratio of AC:EA: maleic acid of 6:5:2

From figure 6, the swelling capacity of HCE-2 hydrogel increased from a mean $370.0 \pm 2.0\%$ to a maximum capacity of $860.0 \pm 5.0\%$ when the mass of AC was increased from 1.0 g to 6.0 g. The increased hydrogel swelling capacity may be attributed to the increased net charges of carboxylate ions in the polymer network which promoted the copolymer's chain expansion [33]. From a mean of $860.0 \pm 5.0\%$, the swelling capacity decreased to $750.0 \pm 2.0\%$ with an increase in the dose of AC monomer to 10.0 g. This may be as a result of increased interactions between amine groups and increasing carboxylate groups resulting in decreased desorption in HCE-2 hydrogel [33]. The decreased swelling percentage capacity was also associated with the bridging effect of the primary amides and increasing electrostatic repulsion of the increased carboxylate groups in HCE-2 hydrogel forcing conformational changes in super hydrogel [2]. The optimal ratio of AC to Ethylenediamine dose for maximum water absorption capacity was found to be 6: 5.

3.5. Effect of Amount of Maleic Acid (g) Used on the Swelling Capacity of Hydrogel (HCE-2)

Figure 7 shows the effect of varying amount of maleic acid cross linker on the mean swelling capacity of super absorber hydrogel HCE-2.

A steady increase in the mean percentage swelling capacity of HCE-2 hydrogel from 330.0 ± 1.0 to $1070.3 \pm 5.0\%$ was noted when the cross linker mass was increased from 0.5 to 2.0 g. Hydrogels with a lower mass of cross linker are flexible with a larger network of pores which facilitates high absorption of water while higher cross linker concentration forms hydrogels with rigid and smaller network sizes of pore shielding water absorption [34]. The percentage decrease in the mean swelling ability of the gel from 1070.3 ± 5.0 to $510.7 \pm 1.2\%$ was noted as the mass of cross linker ratio to that of monomers increased above 2.0 (Figure

7). This could be attributed to the fact that the over cross-linking hinders the mobility of polymeric chains thus lowering the swelling of hydrogel [34]. A mass ratio of AC: EA: maleic acid of 6:5:2 gave the highest mean swelling capacity of $1070.3 \pm 5.0\%$. A chemical cross-linker is important in improving both the integrity of the gel and the predictability of its mechanical properties [35].

3.6. Effect of Swelling Time on the Swelling Capacity of the Hydrogel

Figure 8 shows the effect of swelling time on the swelling capacity of super absorbent hydrogels HCE-2 at different contact times.

From figure 8, the mean percentage swelling increased steadily from $179.7 \pm 4.0\%$ to $1089.7 \pm 0.6\%$ within the first 12 hours and remained constant an indication it had attained its mean maximum swelling capacity. After the optimum swelling time, the porous network of the polymer gel gets saturated with water hence no vacant spaces for more water molecules to occupy [36]. The results show that HCE-2 superabsorbent hydrogel is more hydrophilic due to the presence of hydrogen bond between the carboxylate ions in AC and amine groups in polyamine facilitating water absorption. Jafari and Hamid [37] reported swelling percentage of 850% at pH 7.0 for PAA-based complex. The high swelling capacity of HCE-2 makes it a potential hydrogel for agricultural applications.

4. Conclusions

The results from this study showed that a mass ratio of 6:5:2 between AC with ethylenediamine and maleic acid produced hydrogel with maximum water absorption as well as swelling capacity. The FT-IR spectra sharp bands at 1216.2 cm^{-1} in HCE-1 a credited to N-H bending bond is

proof of interlink between AC and EA monomers. Increased number of -OH functional groups coupled with a sharp peak at 1655.98 cm^{-1} associated with CO stretching in amide, showed successful ester crosslinking in HCE-2 hydrogel during the synthesis process. XRD analysis showed an increased crystallinity in HCE-2 polymer as compared to the amorphous structure in HCE-1 hydrogel. SEM analysis of showed crystalline intact and rigid structure in HCE-1 with fewer pores on their surface compared to the well-developed fibrous with smooth irregular pores and lamina structure in HCE-2. A maximum mean swelling capacity of $1089.7 \pm 0.6\%$ of HCE-2 when subjected to a contact time of 12 hours in 500 mL deionized water was achieved. HCE-2 being a good water absorber has greater potential in boosting agriculture, especially in arid and semi-arid regions by improving water retainability in soils during dry periods.

Declaration of Interests

The authors declare that they have no known competing financial interests or personal relationships that could appear to have influenced the work described in this paper.

ACKNOWLEDGEMENTS

The authors' expresses gratitude to the department of chemistry of Kenyatta University and department of science technology and engineering of Kibabii University for assistance offered during the research period.

REFERENCES

- [1] Słoniewska, A. and Pałys, B. (2014). Supramolecular polyaniline hydrogel as a support for urease, *Electrochimica Acta*, 126: 90–97.
- [2] Gandini, A., Lacerda, T., Carvalho, A., and Trovatti, E. (2016). Progress of Polymers from Renewable Resources: Furans, Vegetable Oils, and Polysaccharides. *Chemistry Review*, 116(3): 1637–1669.
- [3] Koetting, M., Peters, J., Steichen, S. and Peppas, N. (2015). Stimulus-responsive hydrogels: Theory, modern advances, and applications. *Material Science Engineering Research*, 93: 1–49.
- [4] Guilherme, M., Aouada, F., Fajardo, A., Martins, A., Paulino, A., Davi, M., Rubira, A., and Muniz, E. (2015). Superabsorbent hydrogels based on polysaccharides for application in agriculture as soil conditioner and nutrient carrier: A review. *European Polymer Journal*, 72: 365–385.
- [5] Khan, M. and Lo, I. (2016). A holistic review of hydrogel applications in the adsorptive removal of aqueous pollutants: Recent progress, challenges, and perspectives. *Water Research*, 106: 259–271.
- [6] Wang, P., Cao, M., Wang, C., Ao, Y., Hou, J. and Qian, J. (2014). Kinetics and thermodynamics of adsorption of methylene blue by a magnetic graphene-carbon nanotube composite, *Applied Surface Science*, 290: 116–124.
- [7] Senna, A., do-Carmo, J., da-Silva, J., and Botaro, V. (2015). Synthesis, characterization and application of hydrogel derived from cellulose acetate as a substrate for slow-release NPK fertilizer and water retention in soil, *Journal of Environmental Chemical Engineering*, 3(2): 996–1002.
- [8] Farris, S., Schaich, K., Liu, L., Piergiovanni, L., and Yam, K. (2009). Development of polyion-complex hydrogels as an alternative approach for the production of bio-based polymers for food packaging applications: a review. *Trends in Food Science & Technology*, 20(8): 316–332.
- [9] Meng, Y. and Ye, L. (2017). Synthesis and swelling property of superabsorbent starch grafted with acrylic acid/2-acrylamido-2-methyl-1-propanesulfonic acid, *Journal Science Food Agricultural*, 97(11): 3831–3840.
- [10] Ma, J., Li, X. and Bao, Y. (2015). Advances in cellulose-based superabsorbent hydrogels, *Journal of Materials in Civil Engineering*, 5(73): 59745–59757.
- [11] Papita, S. (2010). Assessment on the removal of methylene Blue Dye using Tamarid Fruit Shell as Biosorbent. *Springer Science and Business Media*, 213: 287–299.
- [12] Basri, S.N.; Zainuddin, N.; Hashim, K. and Yusof, N. (2020). Preparation and characterization of irradiated carboxymethyl sago starch-acid hydrogel and its application as metal scavenger in aqueous solution. *Carbohydrate Polymer*, 138: 34–40.
- [13] Demitri, C., Delsole, R., Scalera, F., Sannino, A., Vasapollo, G., Maezzoli, A., Ambrosio, L. and Nicolais, L. (2008). Novel superabsorbent cellulose-based hydrogels cross-linked with citric acid, *Journal of Applied Polymer Science*, 110: 2453–2460.
- [14] Hammond, P., Ali, D. and Cumming, R. (2005). A system on chip digital pH meter for use in a wireless diagnostic capsule. *Biomedical Engineering*, 4: 687–694.
- [15] Wanrosli W. D., Rohaizu R., and Ghazali, A. (2011). Synthesis and characterization of cellulose phosphate from oil palm empty fruit bunches, *Carbohydrate Polymers*, 84: 262–267.
- [16] Zhu, S., Wang, J., Yan, H., Wang, Y., Zhao, Y., Feng, B., Duan, K., and Weng, J. (2017). An injectable supramolecular self-healing bio-hydrogel with high stretchability, extensibility and ductility, and a high swelling ratio, *Journal of Material Chemistry*, 5: 7021.
- [17] Kono, H., and Fujita, S. (2012). Biodegradable superabsorbent hydrogels derived from cellulose by esterification crosslinking with 1, 2, 3, 4-butanetetracarboxylic dianhydride. *Carbohydrate Polymers*, 87(4): 2582–2588.
- [18] Gupta, V. K. and Rastogi, A. (2013). Biosorption of lead from aqueous solutions by green algae *Spirogyra* species: kinetics and equilibrium studies, *Journal of Hazardous Materials*. 152: 407–414.
- [19] Yeasmin, M. S. and Mondal M. I. H. (2015). Synthesis of highly substituted carboxymethyl cellulose depending on cellulose particle size, *International Journal of Biological Macromolecules*, 80: 725–731.
- [20] Merkel, K., H. Rydarowski, J. and Kazimierczak Bloda, A.

- (2014). Processing and characterization of reinforced polyethylene composites made with lignocellulosic fibres isolated from waste plant biomass such as hemp composition. *Journal of Engineering*, 67: 138-144.
- [21] Jiang, W., Saxena A., Song, B., Beveridge T. and Myneni, S. (2004). Elucidation of functional groups on Gram-positive and Gram-negative bacterial surfaces using infrared spectroscopy. *Langmuir*, 20: 11433–11442.
- [22] Parikh, S. and Chorover, J. (2005). FT-IR spectroscopic study of biogenic Mn oxide formation by *Pseudomonas putida* GB-1. *Journal of Geo microbial*, 22: 207-218.
- [23] Capanema, N. S. V., Mansur, A. A. P., De Jesus, A. C., Carvalho, S. M., de Oliveira, L. C., and Mansur, H. S. (2018). Superabsorbent cross-linked carboxymethyl cellulose-PEG hydrogels for potential wound dressing applications. *International Journal of Biological Macromolecules*, 106: 1218–1234.
- [24] Olsson, E., Hedenqvist, M., Johansson, C. and Järnström, L. (2013). Influence of citric acid and curing on moisture sorption, diffusion and permeability of starch films. *Carbohydrate Polymer*, 94(2): 765-772.
- [25] Teodorescu, M., Morariu, S., Bercea, M. and Sacarescu, L. (2016). Viscoelastic and structural properties of poly (vinyl alcohol)/ poly (vinylpyrrolidone) hydrogels.
- [26] Mohamood, N., Zainuddin, N., Ahmad, M. and Tan, S. (2018). Preparation, optimization and swelling study of carboxymethyl sago starch (CMSS)–acid hydrogel. *Chemical Cent. Journal*, 12: 1–10.
- [27] Varaprasad, K., Mohan, Y., Ravindra, S., Reddy, N., Vimala, K., Monika, K., Sreedhar, B. and Raju, K. (2010). Hydrogel-silver nanoparticle composites: A new generation of antimicrobials. *Journal of Applied Polymer Science*, 115: 1199-1207.
- [28] Busselez, R., Arbe, A., Cervený, S., Capponi, S., Colmenero, J. and Frick B. (2012). Component dynamics in polyvinylpyrrolidone concentrated aqueous solutions. *Journal of chemical and physical Chemistry Research* 137: 084902.
- [29] Ou, S., Wang, Y., Tang, S., Huang, C. and Jackson, M. (2005). Role of ferulic acid in preparing edible films from soy protein isolate. *Journal of Food Engineering*, 70: 205-210.
- [30] Kumar, R., Mudhoo, A., Lofrano, G. and Chandra, M. (2014). Adsorbent modification and activation methods and adsorbent regeneration: Biomass-derived biosorbents for metal ions sequestration, *Journal of Environmental Chemical Engineering*, 2: 239-259.
- [31] Lu, S.G., Bai, S. Q., Zhu, L. and Shan, H. D. (2009). Removal mechanism of phosphate from aqueous solution by coal fly ash, *Journal of Hazardous Materials*, (161): 95-101.
- [32] Luo, Y. L., Wei, Q. B., Xu, F., Chen, Y. S., Fan, L. H. and Zhang, C. H. (2009). Assembly, characterization and swelling kinetics of Ag nanoparticles in PDMAAg-PVA hydrogel networks, *Material Chemical Physics*, 118(2-3): 329-336.
- [33] Jyothi Alummoottil, N., Sreekumar, J., Moorthy Subramoney, N., and Sajeew Moothandaserry, S. (2010). Response Surface Methodology for the Optimization and Characterization of Cassava Starch-graft-Poly (acrylamide), *StarchStärke*, 62(1): 18-27.
- [34] Katime, I. and Mendizábal, E. (2010). Swelling Properties of New Hydrogels Based on the Dimethyl Amino Ethyl Acrylate Methyl Chloride Quaternary Salt with Acrylic Acid and 2-Methylene Butane-1,4-Dioic Acid Monomers in Aqueous Solutions. *Materials Sciences and Applications*, 1(03): 162-167.
- [35] Xiao, H. X., Lin, Q.L., Liu, G.Q. and Yu, F. X. (2012). A comparative study of the characteristics of cross-linked, oxidized and dual-modified rice starches. *Molecules*, 17(9): 10946–10957.
- [36] Vimala, K., Sivudu, K. S., Mohan, Y. M., Sreedhar, B. and Raju, K. M. (2009). Controlled silver nanoparticles synthesis in semi-hydrogel networks of poly (acrylamide) and carbohydrates: A rational methodology for antibacterial application. *Carbohydrate Polymer*, 75(3): 463-471.
- [37] Jafari, S. and Hamid, M. (2005). A study on swelling and complex formation of acrylic acid and methacrylic acid hydrogels with polyethylene glycol. *Iran Polymer Journal* 14: 863–873.